https://doi.org/10.5194/bg-2019-391
Preprint. Discussion started: 11 October 2019
© Author(s) 2019. CC BY 4.0 License.

Biogeosciences Discussions
Open Access
EGU

Predominance of hexamethylated 6-methyl branched glycerol dialkyl glycerol tetraethers in the Mariana Trench: Source and environmental implication

Wenjie Xiao[1], Yasong Wang[1], Yongsheng Liu[1], Xi Zhang[1], Linlin Shi[1], Yunping Xu[1*]

[1] Shanghai Engineering Research Center of Hadal Science & Technology, College of Marine Sciences, Shanghai Ocean University, Shanghai 201306, China

***Correspondence**. Yunping Xu (ypxu@shou.edu.cn)

Abstract. Branched glycerol dialkyl glycerol tetraethers (brGDGTs) are useful molecular indicators for organic carbon (OC) source and paleoenvironment. Their application in marine environments, however, is complicated because of the mixed terrestrial and marine contributions to brGDGTs. Here, we employ two dimensional (2D) ultrahigh-performance liquid chromatography-mass spectrometry (UHPLC-MS) to analyze brGDGTs in sediments from the Challenger Deep, Mariana Trench, the deepest ocean in the absent of terrestrial influence. The unique feature is the absence of 5-methyl brGDGTs, and the strong predominance of hexamethylated 6-methyl brGDGT (IIIa') (73.4±2.4% of total brGDGTs). The brGDGTs-reconstructed pH is 8.22±0.07, close to seawater pH. This, combined with characteristics of $\delta^{13}C$ (–19.82±0.25‰), OC/TN ratio (6.72±0.84), branched and isoprenoid tetraether (BIT) index (0.03±0.01) and the acyclic hexa-/pentamethylated brGDGTs ratio (7.13±0.98), strongly suggest that brGDGTs are of autochthonous products from benthic bacteria or planktonic bacteria. The compiling of literature data reveals that enhanced fractional abundance of hexamethylated 6-methyl brGDGTs is common in diverse continental margins when the marine influence became intensified. This may reflect an adaption of brGDGTs-producing bacteria to weak alkaline seawater and low ambient temperature. Based on the global dataset, the cross plot of acyclic hexa-/pentamethylated brGDGTs ratio and fractional abundance of brGDGT-IIIa' is an effective approach to distinguish the terrestrial vs. marine provenance of brGDGTs.

1. Introduction

Glycerol dialkyl glycerol tetraethers (GDGTs) are widely distributed biomarkers in terrestrial and marine settings (Schouten et al., 2013 and references therein). There are two major types of GDGTs, isoprenoidal GDGTs (iGDGTs) and branched GDGTs (brGDGTs) (Sinninghe Damsté et

https://doi.org/10.5194/bg-2019-391
Preprint. Discussion started: 11 October 2019
© Author(s) 2019. CC BY 4.0 License.

al., 2000; Weijers et al., 2006). IGDGTs containing isoprenoid carbon skeleton are biosynthesized by archaea such as Thaumarchaeota, Crenarchaeota and Euryarchaeota (Sinninghe Damsté et al., 2002; Schouten et al., 2008; Knappy et al., 2011; Lincoln et al., 2014). In contrast, brGDGTs consisting of 4–6 methyl groups and 0–2 cyclopentane moieties are biosynthesized by certain bacteria including, but not limit to, Acidobacteria (Sinninghe Damsté et al., 2011). These bacteria are able to alter the degree of methylation and cyclization of brGDGTs with changing ambient environmental conditions (Weijers et al., 2007b). A survey for global soils reveals that the Cyclization of Branched Tetraethers (CBT) correlates with soil pH, while the Methylation of Branched Tetraethers (MBT) is dependent on mean annual air temperature (MAT) and to less extent on soil pH (Weijers et al., 2007b; De Jonge et al., 2014a), leading to the development of brGDGTs-based MBT/CBT proxies for paleo-pH and MAT. The concentration of brGDGTs is substantially higher in peats and soils than marine sediments, and generally decreases from coastal to distal marine sediments (Hopmans et al., 2004; Schouten et al., 2013). These distribution patterns support that brGDGTs in marine settings is derived from terrestrial (particularly soil) inputs. Consequently, the Branched vs. Isoprenoid Tetraether (BIT) index was proposed for estimation of terrestrial (soil) OC in marine sediments (Hopmans et al., 2004).

For the past two decades, the brGDGT-derived proxies such as BIT, MBT and CBT have been increasingly used to assess OC source (Herfort et al., 2006; Kim et al., 2006; Loomis et al., 2011; Wu et al., 2013), soil pH and MAT in a diverse of environments (Weijers et al., 2007a; Sinninghe Damsté et al., 2008; Peterse et al., 2012; Yang et al., 2014). However, the weakness of brGDGTs-based proxies is their source uncertainty. Although brGDGTs were assumed to be specific for soil/peat bacteria, distinct compositions of brGDGT in rivers (Zhang et al., 2012; Zell et al., 2013; Zell et al., 2014a), lakes (Sinninghe Damsté et al., 2009; Tierney and Russell, 2009; Loomis et al., 2011; Buckles et al., 2014), marine waters (Liu et al., 2014; Xie et al., 2014; Zell et al., 2014b) and sediments (Peterse et al., 2009; Zhu et al., 2011; Xiao et al., 2016) support multiple sources of brGDGTs.

The employment of one liquid chromatography (LC) column identified nine individual brGDGTs, all of which were assigned as 5-methyl brGDGTs (Schouten et al., 2007). By improving the performance of liquid chromatographic separation, De Jonge et al. (2013) found that the peaks

https://doi.org/10.5194/bg-2019-391
Preprint. Discussion started: 11 October 2019
© Author(s) 2019. CC BY 4.0 License.


previously identified as 5-methyl brGDGTs were actually the coeluted mixtures of 5-methyl and 6-methyl brGDGTs (3 hexa- and 3 pentamethylated 6-methyl brGDGTs). As a result, the number of identified brGDGTs increases from 9 to 15, which are further expanded after identification of 7-methyl brGDGTs and other isomers (Ding et al., 2016). The analytical improvement has opened the window for the redefinition and recalibration of brGDGT-based proxies and reassessment of brGDGT sources (De Jonge et al., 2014a; Xiao et al., 2015). Adopting the new chromatographic method, several studies provide the clues of in-situ production of brGDGTs in rivers (De Jonge et al., 2014b; De Jonge et al., 2015), lakes (Weber et al., 2015; Weber et al., 2018) and marine sediments (De Jonge et al., 2016; Sinninghe Damsté, 2016). For example, De Jonge et al. (2014b) found that the brGDGT distribution in suspended particulate matter (SPM) of the Yenisei River is fairly constant and characterized by high abundance of brGDGT-IIIa', which were different from that in surrounding soils. An extended study also by De Jonge et al. (2015) showed a marked shift of brGDGTs' compositions from SPM of the Yenisei River to sediments of the Kara Sea. Sinninghe Damsté (2016) reported brGDGTs in surface sediments from the Berau River delta (Kalimantan, Indonesia), and suggested in-situ brGDGT production in coastal settings based on the number of cyclopentane rings ($\#ring_{tetra}$). It should be pointed out that all these studies paid attention to rivers and continental margins (e.g., De Jonge et al., 2015; Sinninghe Damsté, 2016; Warden et al., 2016), where the multiple sources and complex processes make difficulty in discerning allochthonous terrestrial vs. autochthonous marine contributions to the brGDGT pool. Therefore, open ocean in absence of terrestrial influence is an ideal venue for assessment of source and characters of brGDGTs in marine settings.

Here, we choose the Challenger Deep, Mariana Trench to analyze brGDGTs in marine sediments. This deepest trench (ca. 11000 m) is remote from any mainland, and has no significant terrestrial influence (Jamieson, 2015). Our goals are two folds: 1) to determine the composition and concentration of brGDGTs in the Mariana Trench sediments and constrain their source; and 2) to characterize in-situ produced brGDGTs in marine sediments and assess their environmental implication at the global scale by compiling literature data.

2. Material and methods

https://doi.org/10.5194/bg-2019-391
Preprint. Discussion started: 11 October 2019
© Author(s) 2019. CC BY 4.0 License.

88 **2.1 Study area and sampling**

89 The Mariana Trench is formed as the subduction of Pacific plate beneath the eastern edge of
90 the Philippine Sea plate. It has a total length of ca. 2500 km and a mean width of 70 km (Fryer,
91 1996). The deepest point, the Challenger Deep, is located in southern rim of the Mariana Trench
92 and has the water depth of ca. 11000 m. Owing to high current speeds and variable current directions,
93 sediment erosion and/or resuspension at the sediment-water interface may frequently occur (Taira
94 et al., 2004; Turnewitsch et al., 2014). The Mariana Trench is remote from the landmass and located
95 in the extremely oligotrophic Pacific Gyre with annual primary production rate of ca. 59 g C m^{-2} y^{-1}
96 (Jamieson, 2015). Consequently, the sinking fluxes of particulate OC is low. However, the
97 sediment of the Challenger Deep was found exhibiting intensive, microbially-mediated
98 biogeochemical recycling processes relative to that of adjacent abyssal plains (Glud et al., 2013).
99 Such character has been attributed to unique "V"-shaped geometry, intense seismic activity and
100 high-frequency fluid dynamics within the trench that promotes lateral transport of sediments from
101 surrounding shallow regions and accumulation of sedimentary organic matter in trench bottom
102 (Jamieson, 2015; Xu et al., 2018).

103 During an expedition aboard RV Zhangjian (Dec. 2016 to Feb. 2017), a sediment core (MT1,
104 11.43 °N, 142.36 °E, water depth 10840 m, core length 11 cm) was retrieved in the Challenger Deep
105 using an autonomous 11000 m-rated lander (Fig. 1). The core was immediately stored at –20 ºC in
106 a dark room on board until transported to the laboratory in Shanghai (China) where the core was
107 sliced at 1–2 cm interval and kept in a –25 ºC freezer. Prior to analysis, all sliced sediment samples
108 (n = 10) were freeze dried at –40 °C and homogenized by steel spatulas.
109
110 **2.2 Lipid extraction and GDGT analyses**

111 Sediment samples (0.5–2 g) were mixed with known amount of C_{46} GDGTs (internal standard)
112 and 15 ml of mixed dichloromethane/methanol (3:1 v/v). After ultrasonically extracted for 15 min,
113 the extracts were centrifuged (3000 rpm, 5 min) and the supernatants were decanted into clean flasks.
114 The extraction was repeated three times. The combined extracts were concentrated by a Rota
115 Evaporator and further blown down to dryness under mild nitrogen streams. The total lipid extract
116 was dissolved in hexane/isopropanol (99:1, v/v) and filtered through a 0.45 μm PTFE filter prior to

https://doi.org/10.5194/bg-2019-391
Preprint. Discussion started: 11 October 2019
© Author(s) 2019. CC BY 4.0 License.

analysis. An Agilent ultrahigh performance liquid chromatography-atmospheric pressure chemical ionization–triple quadruple mass spectrometry system (UHPLC-APCI-MS) was used. The separation of 5- and 6-methyl brGDGTs was achieved with two silica LC columns in sequence (150 mm × 2.1 mm; 1.9 μm, Thermo Finnigan; USA). The concentration of individual GDGTs was determined by comparison of the respective protonated ion peak areas with C_{46} GDGT in a selected ion monitoring (SIM) mode. The protonated ions were m/z 1050, 1048, 1046, 1036, 1034, 1032, 1022, 1020 and 1018 for brGDGTs, 1302, 1300, 1298, 1296 and 1292 for iGDGTs and 744 for C_{46} GDGT.

2.3 GDGT-derived parameters

The BIT index, an abundance ratio of acyclic hexa- to pentamethylated brGDGTs and the weighted average number of cyclopentane moieties for the tetramethylated brGDGTs ($\#rings_{tetra}$) were calculated according to the definitions of Hopmans et al. (2004), Xiao et al. (2016) and Sinninghe Damsté (2016), respectively. The roman numbers denote relative abundance of GDGTs that are depicted in Fig. 2.

$$BIT=(Ia+IIa+IIIa+IIa'+IIIa')/(Ia+IIa+IIIa+IIa'+IIIa'+Cren) \quad (1)$$

$$\sum IIIa / \sum IIa = (IIIa+IIIa')/(IIa+IIa') \quad (2)$$

$$\#rings_{tetra}=(Ib+2*Ic)/(Ia+Ib+Ic) \quad (3)$$

pH was reconstructed using the CBT' index, while MAT was calculated according to the definition of a Multiple linear Regression-based MAT (MAT_{mr}) (De Jonge et al., 2014a).

$$CBT'=\log[(Ic+IIa'+IIb'+IIc'+IIIa'+IIIb'+IIIc')/(Ia+IIa+IIIa)] \quad (4)$$

$$MAT_{mr}=7.17+17.1*Ia+25.9*Ib+34.4*Ic-28.6*IIa \quad (5)$$

2.4 Bulk geochemical analysis

About 1–2 g of each sediment sample was treated with 1 N HCl for three days at room temperature to remove carbonates, rinsed into neutral pH and freeze-dried. After homogenized with an agate mortar and pestle, approximately 35–40 mg of decarbonated sediments were weighed and analyzed using a model 100 isotope ratio mass spectrometer (IsoPrime Corporation, Cheadle, UK) and a Vario ISOTOPE cube elemental analyzer (Elementar Analysensystem GmbH, Hanau,

https://doi.org/10.5194/bg-2019-391
Preprint. Discussion started: 11 October 2019
© Author(s) 2019. CC BY 4.0 License.

Germany). All isotopic data were reported in δ notation relative to VPDB. The intra-lab standards for normalizing stable carbon isotopic composition ($\delta^{13}C$) was USG24 (Graphite, –16.05‰), which was obtained from the International Atomic Energy Agency (IAEA, Vienna, Austria). The average standard deviation of each measurement, determined by replicate analyses of two samples, was ±0.004 wt% for organic carbon (OC) content, ±0.031 wt% for total nitrogen (TN) content and ±0.03‰ for $\delta^{13}C$.

2.5 Literature data compilation

The dataset in this study is composed of relative abundance of brGDGTs from 2031 samples, including 634 soil samples, 473 peat samples, 88 river samples, 410 lake samples and 426 marine samples (Fig. 1). The detailed information about these samples was listed in supplementary material. The soil samples are from globally distributed soils (De Jonge et al., 2014a; Ding et al., 2015; Xiao et al., 2015; Yang et al., 2015; Lei et al., 2016; Wang et al., 2016; Li et al., 2018; Wang et al., 2018; Zang et al., 2018; Wang et al., 2019). The peat samples are from 96 different peatlands around the world (Naafs et al., 2017). The river samples are from Danube River (Freymond et al., 2016), Yenisei River (De Jonge et al., 2015) and Tagus River (Warden et al., 2016). The lake samples are from East African lakes (Russell et al., 2018), Chinese lakes (Dang et al., 2016; Li et al., 2017; Dang et al., 2018), Lake St Front (Martin et al., 2019), Lake Lugano and other lakes in the European Alps (Weber et al., 2018). The marine samples are from Atlantic Ocean (Warden et al., 2016), Kara Sea (De Jonge et al., 2015; De Jonge et al., 2016), Berau River delta (Sinninghe Damsté, 2016), Ceará Rise (Soelen et al., 2017), North Sea (Dearing Crampton-flood et al., 2018), and Mariana Trench in this study. The criteria for citing the literature data is that both 5- and 6-methyl brGDGTs should be separated and quantified. It is noted that two studies (Weber et al., 2018; Martin et al., 2019) have analyzed 5-, 6- and 7-methyl brGDGTs. But due to very limited reports for 7-methyl brGDGTs, these compounds are not included in this study.

2.6 Statistical analysis

The SPSS package 22 (IBM, USA) was used for statistical analyses including Pearson correlation coefficient (r) and one-way Analysis of Variance (ANOVA). The significance level was

https://doi.org/10.5194/bg-2019-391
Preprint. Discussion started: 11 October 2019
© Author(s) 2019. CC BY 4.0 License.

175 set at $P < 0.05$ unless stated elsewhere.

176

177 **3. Results**

178 **3.1 Bulk geochemical parameters**

179 The OC content, TN content, molar ratio of OC and TN content (OC/TN) and $\delta^{13}C$ value of
180 sediments from the Challenger Deep are summarized in Table 1. The OC and TN contents of
181 sediments vary between 0.26% and 0.31% (0.28±0.01%; mean±STD; same hereafter) and between
182 0.04% and 0.06% (0.05±0.01%), respectively. The OC/TN and $\delta^{13}C$ values range from 5.62 to 8.34
183 (6.72±0.84) and –19.47‰ to −20.27‰ (–19.82±0.25%), respectively. Both the $\delta^{13}C$ and OC/TN
184 values are comparable to previously reported data for the southern Mariana Trench rim and slope
185 ($\delta^{13}C$, –20.48±0.88%; OC/TN, 7.00±1.76) (Luo et al., 2017).

186

187 **3.2 Concentration and composition of GDGTs in the Mariana Trench**

188 The concentration of iGDGTs and brGDGTs are summarized in Table 2. The summed
189 concentration of total GDGTs in sediments of the Mariana Trench varies from 574 to 1162 ng g^{-1}
190 dry weight sediment (dws) (873±166 ng g^{-1} dws), corresponding to 308±56 μg g^{-1} OC. The
191 crenarchaeol is the dominant GDGTs at the concentration of 353 to 667 ng g^{-1} dws (533±99 ng g^{-1}
192 dws), corresponding to 188±33 μg g^{-1} OC. The concentration of brGDGTs ranges from 11 to 18 ng
193 g^{-1} dws (15±3 ng g^{-1} dws), corresponding to 5±1 μg g^{-1} OC and much lower than the concentration
194 of iGDGTs. As a result, the BIT index is low in all samples with an average value of 0.03±0.01.

195 Our improved chromatography has achieved a full separation of 5- and 6-methyl brGDGTs.
196 Interestingly, only a single peak was detected on the mass chromatogram of acyclic penta- (m/z
197 1036) and hexamethylated (m/z 1050) brGDGTs (Fig. 3). This feature is distinct difference from
198 previous studies that have identified two or more peaks (5-methyl, 6-methyl and even 7-methyl
199 isomers) (e.g., De Jonge et al., 2013; Xiao et al., 2015; Ding et al., 2016). In order to determine the
200 structure of brGDGTs in the Mariana Trench sediments, we take advantage of an acidic soil sample
201 from China (Soil-1). This sample was identified to contain both 5-methyl brGDGTs (major) and 6-
202 methyl brGDGTs (minor) (Xiao et al., 2015), and have the IIIa/IIIa' and IIa/IIa' ratios of 12.5 and
203 8.2, respectively (Fig. 3a, b). After combining Soil-1 (soil) and MT-4 (Mariana Trench), two peaks

https://doi.org/10.5194/bg-2019-391
Preprint. Discussion started: 11 October 2019
© Author(s) 2019. CC BY 4.0 License.


were detected for m/z 1050 (hexamethylated brGDGTs) as well as m/z 1036 (pentamethylated brGDGTs) (Fig. 3e, f). The comparison of retention time among Soil-1, MT-4 and the combined sample of Soil-1 and MT-4 shows that the peaks of m/z 1050 and 1036 in the MT-1 are pentamethylated 6-methyl brGDGTs (IIa') and hexamethylated 6-methyl brGDGTs (IIIa'), respectively, eluting after 5-methyl brGDGTs from Soil-1 (Fig. 3). This assignment was corroborated by the reduced 5-emthyl/6-methyl brGDGT ratio of the combined sample that is 1.4 for m/z 1050 and 7.4 for m/z 1036 (Fig. 3e, f).

Throughout the sediment core, the brGDGTs are constantly dominated by 6-methyl isomers (82.25–86.91%). The fractional abundance of 5-methyl brGDGTs, however, was too low to be quantified. For individual compounds, brGDGT-IIIa' is the most abundant (73.40±2.39% of total brGDGTs), followed by brGDGT-Ia (12.46±1.14%) and brGDGT-IIa' (10.45±1.20%). The cyclic compounds (brGDGT-Ib, Ic, IIb') are minor constituents of the brGDGTs (3.69±0.75%), resulting in low $\#rings_{tetra}$ values (0.26±0.04). The classification based on the number of methyl groups shows the dominance of hexamethylated brGDGTs (73.53±2.56%) over tetramethylated (15.43±1.53%) and pentamethylated (11.04±1.49%) brGDGTs.

4. Discussion

4.1 In-situ production of 6-methyl brGDGT in the Mariana Trench

To the best of our knowledge, there are only two reports about GDGTs in the Mariana subduction zone. Guan et al. (2019) investigated iGDGT distribution in the surface sediments (4900–7068 m) from the southern Mariana Trench, while Ta et al. (2019) analyzed iGDGTs and brGDGTs in two sediment cores (ca. 5400 m) at subduction plate of the Mariana Trench. These two studies, however, did not separate the 5- and 6-methyl brGDGTs, and thus are unable to reveal any information about source and environmental implication of 5- and 6-methyl brGDGTs. In our study, the strong predominance of 6-methyl brGDGTs and the absence of 5-methyl brGDGTs in the Marine Trench sediments are a unique feature. In order to understand the mechanism to produce such unique compositions of brGDGTs, source assessment of brGDGTs is needed.

The multiple lines of evidence from stable carbon isotope, OC/TN ratio and biomarkers unanimously support an in-situ production of brGDGTs in the Mariana Trench. The $\delta^{13}C$ and OC/TN

https://doi.org/10.5194/bg-2019-391
Preprint. Discussion started: 11 October 2019
© Author(s) 2019. CC BY 4.0 License.

ratio have been widely used to distinguish terrestrial vs. marine OC (Meyers, 1997). Generally, marine algae and bacteria are protein-rich and have OC/TN ratio of 4 to 10, whereas vascular land plants are cellulose and lignin-rich and have OC/TN ratio of 20 or greater. Due to different carbon sources and photosynthetic pathways, the typical $\delta^{13}C$ value is ca. –22‰ to –20‰ for marine organisms (Meyers, 1994) and –27‰ for terrestrial C_3 plants (O'Leary, 1988). Sediments from the Mariana Trench yield enriched $\delta^{13}C$ signatures (–19.82±0.25‰) and low OC/TN values (6.72±0.84), suggesting marine phytoplankton/bacteria as a major contributor to sedimentary OC (Fig. 4). This result is expected since the Mariana Trench is remote from the landmasses (Fig. 1) and also agrees with the previous report from Luo et al. (2017).

Long-distance dust transport from continent to open ocean might deliver brGDGTs to the Mariana Trench. Unfortunately, no data is available about brGDGTs of eolian dust in the Mariana Trench region. Weijers et al. (2014) compared the composition of brGDGTs between the marine sediments and atmospheric dust in the equatorial West African coast, and the great difference suggests an in-situ production of brGDGTs in the marine sediments, rather than dust input. Here, we examine the brGDGT compositions in the Mariana Trench sediments with literature data from global environmental settings (Fig. 5). Relative to the Mariana Trench sediments (brGDGT-Ia 12.46±1.14%, 5-methyl brGDGTs ~0, brGDGT-IIIa' 73.40±2.39%), terrestrial samples are characterized by significantly higher proportions of brGDGT-Ia (soil 37.52±25.91%, peat 59.40±21.19%, river 15.38±2.97%) and 5-methyl brGDGTs (soil 23.56±14.83%, peat 34.04±19.18%, river 33.25±8.51%), but lower proportions of brGDGT-IIIa' (soil 4.89±4.82%, peat 4.86±4.68%, river 11.68±4.40%) ($p < 0.005$) (Fig. 5). These terrestrial samples are globally distributed and many of them are from inner Asian continent, the major source area of dust in North Pacific (Husar et al., 2001). Thus, brGDGTs in the Mariana Trench sediments are unlikely derived from air dusts. We note that brGDGTs in the Lake Lugano, a deep meromictic Swiss lake, is also characterized by the strong predominance of brGDGT-IIIa' (up to 90%) (Fig. 5; Weber et al., 2018), where the distributional patterns and $\delta^{13}C$ of brGDGTs support an provenance in the lower part of the oxygenated water column. However, most marine samples in the literature present low proportions of brGDGT-IIIa' (9.61±6.28%), much lower than that of the Mariana Trench sediments. This difference may reflect different terrestrial influences since most marine samples in previous

https://doi.org/10.5194/bg-2019-391
Preprint. Discussion started: 11 October 2019
© Author(s) 2019. CC BY 4.0 License.


studies are from continental margins where significant inputs of terrestrial-derived brGDGTs may mask the marine signal (Hopmans et al., 2004).

Low BIT values (0.03±0.01; Fig. 6) in the Mariana Trench sediments is in similar to distal marine sediments (an average of 0.04) (Schouten et al., 2013; Weijers et al., 2014), suggesting insignificant terrestrial inputs. By compilation of globally distributed 1354 marine sediments and 589 soils, Xiao et al. (2016) found that the (IIIa+IIIa')/(IIa+IIa') ratio was < 0.59 in over 90% of soils and 0.59–0.92 and > 0.92 in marine sediments with and without significant terrestrial inputs, respectively. In this study, the (IIIa+IIIa')/(IIa+IIa') ratio varies between 5.68 and 8.33 (7.13±0.98) (Fig. 6), much higher than the threshold value for marine origin (0.92), supporting in-situ production of brGDGTs in the Mariana Trench sediments.

De Jonge et al. (2014a) proposed a CBT' index to reconstruct the soil pH based on global distributed soils. Combined with new available data, we recalibrated the correlation of soil pH with the CBT' index: $\mathrm{pH}=(1.459 \pm 0.025) \times \mathrm{CBT}'+(7.001 \pm 0.023)$ $(n = 628, \mathrm{R}^2 = 0.84, p < 0.001)$ (Fig. 7a). According to this equation, the CBT' index of the Mariana Trench sediments ranges from 0.78 to 0.90 (0.84±0.05) and the reconstructed pH is 8.22±0.07 (Fig. 7a). This pH is very close to that of weak alkaline seawater (ca. 8.2), and therefore the brGDGTs in the Mariana Trench are most likely produced in the marine environment.

Overall, the characters of bulk geochemical parameters, brGDGT compositions, the BIT index and brGDGT-derived pH of soil and marine samples all support that brGDGTs in Mariana Trench sediments are in-situ products rather than terrestrial inputs.

4.2 High fractional abundance of brGDGT-IIIa' as a common phenomenon in marine environments

Not only Mariana Trench sediments, but also samples from continental margins show relatively high proportions of hexamethylated 6-methyl brGDGTs. Dearing Crampton-flood et al. (2018) explored brGDGTs and bulk properties of organic matter in a sediment record from the North Sea Basin during the period of early Pliocene to early Pleistocene. The OC content, $\delta^{13}C$ value, BIT and $\#\mathrm{rings}_{\mathrm{tetra}}$ index indicate a transition from predominant marine OC during the Pliocene to predominant terrestrial OC in the Pleistocene. Correspondingly, the fractional abundance of

https://doi.org/10.5194/bg-2019-391
Preprint. Discussion started: 11 October 2019
© Author(s) 2019. CC BY 4.0 License.


brGDGT-IIIa' is higher during the Pliocene (8.06±1.92%) than the Pleistocene (5.16±0.83%), and exhibits significant correlations with $\delta^{13}C$ ($R^2 = 0.68$, $p < 0.001$) and the BIT index ($R^2 = 0.46$, $p < 0.001$) (Fig. 8a, b, c). These correlations support that the variation in OC source controls the composition of brGDGTs.

Another supporting evidence is from the Kara Sea. De Jonge et al. (2016) investigated sedimentary brGDGT record of the Kara Sea spanning a minimum of 13.3 ka. The greater marine OC contribution in the shallow sediments (1–130 cm; < 10 ka) was revealed by heavier $\delta^{13}C$ (up to –23‰) and lower BIT index (close to 0) compared to deep sediments (Fig. 8e, f). Coincide with this change, the fractional abundance of GDGT-IIIa' appeared to be increasing from < 5% to 15% (Fig. 8d). Similar to the North Sea Basin, the significant correlations of the fractional abundance of brGDGT-IIIa' with the $\delta^{13}C$ ($R^2 = 0.34$; $p < 0.001$) and the BIT index ($R^2 = 0.50$; $p < 0.001$) were observed in the Kara Sea, again suggesting that marine organisms tend to produce more hexamethylated 6-methyl brGDGTs.

Besides temporal variations in sediment cores, the fractional abundance of 6-methyl brGDGTs also varied spatially in modern samples from land to sea. Warden et al. (2016) examined brGDGTs along a transect from the Tagus River into the deep ocean off the Portuguese margin. From source to sink in the Tagus River basin, the BIT index decreases from 0.9 to < 0.1, reflecting a substantial increase in marine contribution to sedimentary OC pool (Fig. 8h). Meanwhile, the proportion of brGDGT-IIIa' increases from 11.07±2.62% to 29.31±6.45%, and brGDGT-IIIa' became the most abundant compound in the Lower Setúbal Canyon sediments (Fig. 8g). Sinninghe Damsté (2016) reported brGDGT composition in surface sediments from the Berau River delta including two coast-shelf transects, and proposed $\#rings_{tetra}$ index to discern sources of brGDGTs. The $\#rings_{tetra}$ index shows a marked increase from the river mouth (0.22) to the shelf break (0.83). By compiling the data in Sinninghe Damsté (2016), we found that the proportion of brGDGT-IIIa' generally increases seawards, presenting a similar distribution pattern as that of the $\delta^{13}C$ and BIT index (Fig. 8i, j, k). These spatial variations confirm that that marine in-situ production of brGDGTs is characterized by the high fractional abundance of hexamethylated 6-methyl isomer.

In sum, the studies for the Kara Sea (De Jonge et al., 2016), the North Sea Basin (Dearing Crampton-flood et al., 2018), the Tagus River basin (Warden et al., 2016) and the Berau River delta

https://doi.org/10.5194/bg-2019-391
Preprint. Discussion started: 11 October 2019
© Author(s) 2019. CC BY 4.0 License.

(Sinninghe Damsté, 2016) all demonstrate increasing proportion of 6-methyl brGDGTs (particularly IIIa') with intensified marine influence. These findings, along with the strong predominance of brGDGT-IIIa' in the Mariana Trench sediments, suggest that the high proportion of brGDGT-IIIa' is a common phenomenon in marine environments where in-situ production of brGDGTs is significant.

4.3 Potential mechanisms to produce high proportions of brGDGT-IIIa' in marine environments

A survey of brGDGTs in globally distributed soils suggests that brGDGT producing microbes can adjust their membrane lipid compositions in response to environmental conditions, reflected by the increase in cyclization degree of brGDGTs and the shift from 5- to 6-methyl group with increasing pH and decreasing methylation of brGDGTs with temperature (Weijers et al., 2007b; De Jonge et al., 2014a; Ding et al., 2015; Xiao et al., 2015). This adaption mechanism may be extrapolated to marine organisms. In the Mariana Trench, in-situ production yields brGDGTs with the strong predominance of 6-methyl (84.57±1.53%) (Table 2). The cyclopentane-containing brGDGTs (Ib, Ic, IIb, IIb', IIc, IIc', IIIb, IIIb', IIIc, IIIc') comprise only 3.69±0.75% of total brGDGTs, and the $\#rings_{tetra}$ index is low (0.26±0.04). This seems contrast to a view that the fractional abundance of cyclopentane-containing brGDGTs is positively correlated with pH (Sinninghe Damsté, 2016). This discrepancy can be explained by two reasons. First, the isomerization of brGDGTs, relative to the cyclization of brGDGTs, is a more effective way in response to changing pH. Based on global soil dataset, the correlation between the Isomerization of Branched Tetraethers index (IBT; Xiao et al., 2015) and pH is substantially higher ($n = 610$, $R^2 = 0.80$, $p < 0.001$, Fig. 7b) than that between the $\#rings_{tetra}$ index and pH ($n = 631$, $R^2 = 0.46$, $p < 0.001$, Fig. 7d) as well as that between the cyclization index (CBT_{5me}) (De Jonge et al., 2014a) and pH ($n = 622$, $R^2 = 0.67$, $p < 0.001$, Fig. 7c). Meanwhile, the global soils with pH > 8 ($n = 58$) are characterized by higher fractional abundance of 6-methyl brGDGTs (68.22±10.41%) than the cyclopentane-containing brGDGTs (16.69±9.43%). The second explanation is that brGDGT producing microbes tend to produce more hexamethylated brGDGTs at low temperature (Sinninghe Damsté, 2016), thus reducing the relative proportion of cyclic tetramethylated and pentamethylated brGDGTs. Based on

https://doi.org/10.5194/bg-2019-391
Preprint. Discussion started: 11 October 2019
© Author(s) 2019. CC BY 4.0 License.


the global dataset, if we take 100% of tetramethylated brGDGTs as a starting point, a decreasing proportion of tetramethylated brGDGTs, most likely caused by decreasing temperature (Weijers et al., 2007b), is initially compensated by a roughly linear increase of pentamethylated brGDGTs (Fig. 9d) and, to less extent, by a slower increase of hexamethylated brGDGTs (Fig. 9b). However, when tetramethylated brGDGTs decreases to 20% of total brGDGTs, hexamethylated brGDGTs become dominant, whereas pentamethylated brGDGTs reach a turning point and begin to rapidly decrease (Fig. 9b, d). The ternary diagram, plotted with fractional abundance of tera-, penta- and hexa-methylated brGDGTs (Fig. 9), shows that the Mariana Trench sediments have distinct and high fractional abundance of hexamethylated brGDGTs (73.53±2.56%). We thus propose that low temperature and high pH of deep-sea environments are responsible for production of brGDGTs with high degree of methylation and the predominance of 6-methyl brGDGTs, especially brGDGT-IIIa'.

Marine in-situ production of brGDGTs may take place in water column, or sediments, or both. Sinninghe Damsté (2016) suggested in-situ production of brGDGTs is a widespread phenomenon in shelf sediments that is especially pronounced at water depths of ca. 50–300 m. Based on an extended dataset of brGDGTs in open sea sediments (water depth 63–5521 m), the reconstructed pH ranges from 6.1 to 9.9 (Weijers et al., 2014). This indicates that the brGDGTs was mainly produced in benthic sediments where the pH of porewater is more variable than that of the water column. However, the CBT'-derived pH in the Mariana Trench fell in a narrow range (8.22±0.07), which are in line with the pH of the water column. Additionally, the brGDGTs-reconstructed temperature using the MAT_{mr} index ranged from 9.6 to 10.7 °C (10.2±0.3 °C), which is close to the water temperature at ca. 300 m, but much higher than the temperature of benthic sediments (1.2 °C) (Takuro et al., 2015; Tian et al., 2018). Given these facts, in-situ production of brGDGTs can occur in both water column and benthic sediments, although the contribution weight of each sources may be site-specific.

4.4 Deciphering brGDGT provenance in marine sediments

There are increasing concerns about the applicability of the brGDGT-based proxies in continental margins which are characterized by intense land-sea interaction (De Jonge et al., 2016; Sinninghe Damsté, 2016; Dearing Crampton-flood et al., 2018). Determining the provenance of

https://doi.org/10.5194/bg-2019-391
Preprint. Discussion started: 11 October 2019
© Author(s) 2019. CC BY 4.0 License.


brGDGTs is prerequisite for accurate application of brGDGTs-based proxies. Our study highlights that in-situ produced brGDGTs tend to exhibit higher fractional abundance of brGDGT-IIIa' relative to terrestrial brGDGTs in most soil and peat samples. However, the fractional abundance of brGDGT-IIIa' alone cannot decipher soil and marine source of brGDGTs since fractional abundance of brGDGT-IIIa' in soils are variable and can reach up to 51% (De Jonge et al., 2014a). Xiao et al. (2016) proposed the (IIIa+IIIa')/(IIa+IIa') ratio of < 0.59, 0.59–0.92 and > 0.92 to indicate an origin of brGDGTs from soils, marine sediments with terrestrial influence and marine sediments without terrestrial influence, respectively. However, the updated dataset shows some overlaps of the (IIIa+IIIa')/(IIa+IIa') values between soils and marine sediments (Fig. 10). In order to circumvent this problem, we propose a new approach to evaluate the source of brGDGTs based on the slope of the (IIIa+IIIa')/(IIa+IIa') ratio and fractional abundance of brGDGT-IIIa' (Fig. 10). Specifically, the slope of global soils (30.5±0.7) is substantially greater than that of marine sediments with terrestrial influence (8.2±0.1), both of which are substantially greater than the slope of the Mariana Trench sediments without terrestrial influence (2.3±0.3) (Fig. 10). The extremely low slope of Mariana Trench sediments likely suggests that brGDGT are completely derived from in-situ production.

The systematic differences in the composition of brGDGTs between terrestrial and marine production inevitably affect brGDGTs proxies. Since the CBT' index involves brGDGT-IIIa', the marine in-situ production of brGDGTs with higher fractional abundance of brGDGT-IIIa' is very likely to impact the CBT'-pH proxy. Although the brGDGT based temperature proxies, like MBT'_{5me} and MAT_{mr}, do not directly involve brGDGT-IIIa' (De Jonge et al., 2014a), in-situ production of hexamethylated 6-methyl brGDGT will cause changes in proportions of tetra- and pentamethylated brGDGTs to different degrees (Fig. 9b, c), and thereby influence brGDGTs based temperature proxies.

5. Conclusions

This work represents the first study for 5-methyl and 6-methyl brGDGT in sediments from the Mariana Trench, the deepest ocean realm, from which we have reached three conclusions.

1) The Mariana Trench sediments are characterized by the strong predominance of 6-methyl brGDGTs (84.57±1.53% of total brGDGTs), especially brGDGT-IIIa' (73.40±2.39%), whereas 5-

https://doi.org/10.5194/bg-2019-391
Preprint. Discussion started: 11 October 2019
© Author(s) 2019. CC BY 4.0 License.

methyl brGDGTs are below detection limit. This unique feature has never been previously reported and is attributed to a combined effect of the lack of terrestrial input, alkaline seawater and low subsurface temperature in the Mariana Trench.

2) High (IIIa+IIIa')/(IIa+IIa') values (7.13±0.98), enriched $\delta^{13}C$ signatures (–19.82±0.25‰), low OC/TN ratios (6.72±0.84) and low BIT index (0.03±0.01) strongly suggest an in-situ production of brGDGTs. By compiling brGDGT dataset from 634 soil, 473 peat, 88 river, 410 lake and 426 marine samples, we recalibrate the correlation of soil pH with the CBT' index ($R^2 = 0.84$, $p < 0.001$). The reconstructed CBT'-pH (8.22±0.07) is close to weak alkaline seawater, while the MBT_{mr} reconstructed temperature (10.2±0.3 °C) is close to water temperature at ca. 300 m deep, suggesting a principal contribution of planktonic bacteria to the brGDGT pool in the Mariana Trench sediments.

3) BrGDGTs in sediments from the Mariana Trench and several continental margins were found to comprise higher fractional abundance of hexamethylated 6-methyl brGDGTs with intensified marine influence. The slope of fractional abundance of brGDGT-IIIa' and the (IIIa+IIIa')/(IIa+IIa') index can be used to decipher the terrestrial and marine provenance of brGDGTs. Since in-situ production of predominant hexamethylated 6-methyl brGDGT influences the robustness of brGDGT-based proxies, this study provides a new way to estimate brGDGT sources and holds some promise in reducing uncertainty of brGDGTs-based paleoenvironmental proxies.

Data availability: Data have been made available through FIGSHARE: https://doi.org/10.6084/m9.figshare.9896120.v1 (Xiao et al., 2019)

Acknowledgements Samples were obtained during cruises by the RV Zhangjian. We are grateful to captains, crews, and scientific personnel for their excellent support to obtain the samples. Weicheng Cui, Binbin Pan and Jiasong Fang are thanked for their assistance in cruise organization, lander design and instrumental analyses, respectively. The cruise is financially supported by the Shanghai Committee of Science and Technology (15DZ1207000). The additional financial support is from National Natural Science Foundation of China (41976030; 41676058) to Y. Xu.

https://doi.org/10.5194/bg-2019-391
Preprint. Discussion started: 11 October 2019
© Author(s) 2019. CC BY 4.0 License.

435 **References**

436 Buckles, L.K., Weijers, J.W.H., Verschuren, D. and Sinninghe Damsté, J.S. (2014) Sources of core and
437 intact branched tetraether membrane lipids in the lacustrine environment: Anatomy of Lake Challa and
438 its catchment, equatorial East Africa. Geochim. Cosmochim. Acta 140, 106–126,
439 https://doi.org/10.1016/j.gca.2014.04.042.

440 Dang, X., Ding, W., Yang, H., Pancost, R.D., Naafs, B.D.A., Xue, J., Xiao, L., Lu, J. and Xie, S. (2018)
441 Different temperature dependence of the bacterial brGDGT isomers in 35 Chinese lake sediments
442 compared to that in soils. Org. Geochem. 119, 72–79, https://doi.org/10.1016/j.orggeochem.2018.02.008.

443 Dang, X.Y., Xue, J.T., Yang, H. and Xie, S.C. (2016) Environmental impacts on the distribution of
444 microbial tetraether lipids in Chinese lakes with contrasting pH: Implications for lacustrine
445 paleoenvironmental reconstructions. Sci. China Earth Sci. 59, 939–950, https://doi.org/10.1007/s11430-
446 015-5234-z

447 De Jonge, C., Hopmans, E.C., Stadnitskaia, A., Rijpstra, W.I.C., Hofland, R., Tegelaar, E. and Sinninghe
448 Damsté, J.S. (2013) Identification of novel penta- and hexamethylated branched glycerol dialkyl glycerol
449 tetraethers in peat using HPLC–MS^2, GC–MS and GC–SMB-MS. Org. Geochem. 54, 78–82,
450 https://doi.org/10.1016/j.orggeochem.2012.10.004.

451 De Jonge, C., Hopmans, E.C., Zell, C.I., Kim, J.-H., Schouten, S. and Sinninghe Damsté, J.S. (2014a)
452 Occurrence and abundance of 6-methyl branched glycerol dialkyl glycerol tetraethers in soils:
453 Implications for palaeoclimate reconstruction. Geochim. Cosmochim. Acta 141, 97–112,
454 http://dx.doi.org/10.1016/j.gca.2014.06.013.

455 De Jonge, C., Stadnitskaia, A., Cherkashov, G. and Sinninghe Damsté, J.S. (2016) Branched glycerol
456 dialkyl glycerol tetraethers and crenarchaeol record post-glacial sea level rise and shift in source of
457 terrigenous brGDGTs in the Kara Sea (Arctic Ocean). Org. Geochem. 92, 42–54,
458 http://dx.doi.org/10.1016/j.orggeochem.2015.11.009.

459 De Jonge, C., Stadnitskaia, A., Hopmans, E.C., Cherkashov, G., Fedotov, A. and Sinninghe Damsté, J.S.
460 (2014b) In situ produced branched glycerol dialkyl glycerol tetraethers in suspended particulate matter
461 from the Yenisei River, Eastern Siberia. Geochim. Cosmochim. Acta 125, 476–491,
462 https://doi.org/10.1016/j.gca.2013.10.031.

463 De Jonge, C., Stadnitskaia, A., Hopmans, E.C., Cherkashov, G., Fedotov, A., Streletskaya, I.D., Vasiliev,
464 A.A. and Sinninghe Damsté, J.S. (2015) Drastic changes in the distribution of branched tetraether lipids

https://doi.org/10.5194/bg-2019-391
Preprint. Discussion started: 11 October 2019
© Author(s) 2019. CC BY 4.0 License.

in suspended matter and sediments from the Yenisei River and Kara Sea (Siberia): Implications for the use of brGDGT-based proxies in coastal marine sediments. Geochim. Cosmochim. Acta 165, 200–225, https://doi.org/10.1016/j.gca.2015.05.044.

Dearing Crampton-flood, E., Peterse, F., Munsterman, D. and Sinninghe Damsté, J.S. (2018) Using tetraether lipids archived in North Sea Basin sediments to extract North Western European Pliocene continental air temperatures. Earth Planet. Sci. Lett. 490, 193–205, https://doi.org/10.1016/j.epsl.2018.03.030.

Ding, S., Schwab, V.F., Ueberschaar, N., Roth, V.N., Lange, M., Xu, Y., Gleixner, G. and Pohnert, G. (2016) Identification of novel 7-methyl and cyclopentanyl branched glycerol dialkyl glycerol tetraethers in lake sediments. Org. Geochem. 102, 52–58, https://doi.org/10.1016/j.orggeochem.2016.09.009.

Ding, S., Xu, Y., Wang, Y., He, Y., Hou, J., Chen, L. and He, J.S. (2015) Distribution of branched glycerol dialkyl glycerol tetraethers in surface soils of the Qinghai–Tibetan Plateau: implications of brGDGTs-based proxies in cold and dry regions. Biogeosciences 12, 3141–3151, https://doi.org/10.5194/bg-12-3141-2015.

Freymond, C.V., Peterse, F., Fischer, L.V., Filip, F., Giosan, L. and Eglinton, T.I. (2016) Branched GDGT signals in fluvial sediments of the Danube River basin: Method comparison and longitudinal evolution. Org. Geochem. 103, S0146638016303151.

Fryer, P. (1996) Evolution of the Mariana Convergent Plate Margin System. Rev. Geophys. 34, 89–125, https://doi.org/10.1029/95RG03476.

Glud, R.N., Wenzhofer, F., Middelboe, M., Oguri, K., Turnewitsch, R., Canfield, D.E. and Kitazato, H. (2013) High rates of microbial carbon turnover in sediments in the deepest oceanic trench on Earth. Nat. Geosci. 6, 284–288, https://doi.org/10.1038/ngeo1773

Goñi, M.A., Monacci, N., Gisewhite, R., Ogston, A., Crockett, J. and Nittrouer, C. (2006) Distribution and sources of particulate organic matter in the water column and sediments of the Fly River Delta, Gulf of Papua (Papua New Guinea). Estuar. Coast. Shelf Sci. 69, 225–245, https://doi.org/10.1016/j.ecss.2006.04.012.

Guan, H., Chen, L., Luo, M., Liu, L., Mao, S., Ge, H., Zhang, M., Fang, J. and Chen, D. (2019) Composition and origin of lipid biomarkers in the surface sediments from the southern Challenger Deep, Mariana Trench. Geosci. Front. 10, 351–360, https://doi.org/10.1016/j.gsf.2018.01.004.

Herfort, L., Schouten, S., Boon, J.P., Woltering, M., Baas, M., Weijers, J.W.H. and Sinninghe Damsté,

https://doi.org/10.5194/bg-2019-391
Preprint. Discussion started: 11 October 2019
© Author(s) 2019. CC BY 4.0 License.

J.S. (2006) Characterization of transport and deposition of terrestrial organic matter in the southern North Sea using the BIT index. Limnol. Oceanogr. 51, 2196–2205, https://doi.org/10.4319/lo.2006.51.5.2196.

Hopmans, E.C., Weijers, J.W.H., Schefuss, E., Herfort, L., Sinninghe Damsté, J.S. and Schouten, S. (2004) A novel proxy for terrestrial organic matter in sediments based on branched and isoprenoid tetraether lipids. Earth Planet. Sci. Lett. 224, 107–116, https://doi.org/10.1016/j.epsl.2004.05.012.

Hu, L., Shi, X., Bai, Y., Qiao, S., Li, L., Yu, Y., Yang, G., Ma, D. and Guo, Z. (2016) Recent organic carbon sequestration in the shelf sediments of the Bohai Sea and Yellow Sea, China. J. Mar. Syst. 155, 50–58, https://doi.org/10.1016/j.jmarsys.2015.10.018.

Husar, R.B., Tratt, D.M., Schichtel, B.A., Falke, S.R., Li, F., Jaffe, D., Gassó, S., Gill, T., Laulainen, N.S., Lu, F., Reheis, M.C., Chun, Y., Westphal, D., Holben, B.N., Gueymard, C., McKendry, I., Kuring, N., Feldman, G.C., McClain, C., Frouin, R.J., Merrill, J., DuBois, D., Vignola, F., Murayama, T., Nickovic, S., Wilson, W.E., Sassen, K., Sugimoto, N. and Malm, W.C. (2001) Asian dust events of April 1998. J. Geophys. Res. Atmosph. 106, 18317–18330, https://doi.org/10.1029/2000JD900788.

Jamieson, A. (2015) The hadal zone: life in the deepest oceans. Cambridge University Press.

Kim, J.H., Schouten, S., Buscail, R., Ludwig, W., Bonnin, J., Sinninghe Damsté, J.S. and Bourrin, F. (2006) Origin and distribution of terrestrial organic matter in the NW Mediterranean (Gulf of Lions): Exploring the newly developed BIT index. Geochem. Geophys. Geosyst. 7, 220–222, https://doi.org/10.1029/2006GC001306.

Knappy, C.S., Nunn, C.E.M., Morgan, H.W. and Keely, B.J. (2011) The major lipid cores of the archaeon Ignisphaera aggregans: implications for the phylogeny and biosynthesis of glycerol monoalkyl glycerol tetraether isoprenoid lipids. Extremophiles Life Under Extreme Conditions 15, https://doi.org/10.1007/s00792-00011-00382-00793.

Lei, Y., Yang, H., Dang, X., Zhao, S. and Xie, S. (2016) Absence of a significant bias towards summer temperature in branched tetraether-based paleothermometer at two soil sites with contrasting temperature seasonality. Org. Geochem. 94, 83–94, https://doi.org/10.1016/j.orggeochem.2016.02.003.

Li, J., Naafs, B.D.A., Pancost, R.D., Yang, H., Deng, L. and Xie, S. (2017) Distribution of branched tetraether lipids in ponds from Inner Mongolia, NE China: Insight into the source of brGDGTs. Org. Geochem. 112, 127–136, https://doi.org/10.1016/j.orggeochem.2017.07.005.

Li, Y., Zhao, S., Pei, H., Shi, Q., Zang, J., Dang, X. and Yang, H. (2018) Distribution of glycerol dialkyl glycerol tetraethers in surface soils along an altitudinal transect at cold and humid Mountain Changbai:

https://doi.org/10.5194/bg-2019-391
Preprint. Discussion started: 11 October 2019
© Author(s) 2019. CC BY 4.0 License.

Implications for the reconstruction of paleoaltimetry and paleoclimate. Sci. China Earth Sci., 1–15, https://doi.org/10.1007/s11430-017-9168-9.

Lincoln, S.A., Brenner, W., Eppley, J.M., Church, M.J., Summons, R.E. and Delong, E.F. (2014) Planktonic Euryarchaeota are a significant source of archaeal tetraether lipids in the ocean. Proc. Natl. Acad. Sci. USA 111, 9858–9863, https://doi.org/10.1073/pnas.1409439111

Liu, X., Zhu, C., Wakeham, S., G and Hinrichs, K. (2014) In situ production of branched glycerol dialkyl glycerol tetraethers in anoxic marine water columns. Mar. Chem. 166, 1–8, https://doi.org/10.1016/j.marchem.2014.08.008.

Loomis, S.E., Russell, J.M. and Sinninghe Damsté, J.S. (2011) Distributions of branched GDGTs in soils and lake sediments from western Uganda: Implications for a lacustrine paleothermometer. Org. Geochem. 42, 739–751, http://dx.doi.org/10.1016/j.orggeochem.2011.06.004.

Luo, M., Gieskes, J., Chen, L., Shi, X. and Chen, D. (2017) Provenances, distribution, and accumulation of organic matter in the southern Mariana Trench rim and slope: Implication for carbon cycle and burial in hadal trenches. Mar. Geol. 386, 486–498, https://doi.org/10.1016/j.margeo.2017.02.012.

Martin, C., Ménot, G., Thouveny, N., Davtian, N., Andrieu-Ponel, V., Reille, M. and Bard, E. (2019) Impact of human activities and vegetation changes on the tetraether sources in Lake St Front (Massif Central, France). Org. Geochem. 135, 38–52, https://doi.org/10.1016/j.orggeochem.2019.06.005.

Meyers, P.A. (1994) Preservation of elemental and isotopic source identification of sedimentary organic matter. Chem. Geol. 144, 289–302, https://doi.org/10.1016/0009-2541(94)90059-0.

Meyers, P.A. (1997) Organic geochemical proxies of paleoceanographic, paleolimnologic, and paleoclimatic processes. Org. Geochem. 27, 213–250.

Naafs, B.D.A., Inglis, G.N., Zheng, Y., Amesbury, M.J., Biester, H., Bindler, R., Blewett, J., Burrows, M.A., Torres, D.D.C. and Chambers, F.M. (2017) Introducing global peat-specific temperature and pH calibrations based on brGDGT bacterial lipids. Geochim. Cosmochim. Acta 208, 285–301, https://doi.org/10.1016/j.gca.2017.01.038.

O'Leary, M.H. (1988) Carbon isotopes in photosynthesis. Bioscience 38, 328–336, https://doi.org/10.2307/1310735

Peterse, F., Kim, J.-H., Schouten, S., Kristensen, D.K., Koç, N. and Sinninghe Damsté, J.S. (2009) Constraints on the application of the MBT/CBT palaeothermometer at high latitude environments (Svalbard, Norway). Org. Geochem. 40, 692–699, http://dx.doi.org/10.1016/j.orggeochem.2009.03.004.

https://doi.org/10.5194/bg-2019-391
Preprint. Discussion started: 11 October 2019
© Author(s) 2019. CC BY 4.0 License.

555 Peterse, F., van der Meer, J., Schouten, S., Weijers, J.W.H., Fierer, N., Jackson, R.B., Kim, J.H. and
556 Sinninghe Damsté, J.S. (2012) Revised calibration of the MBT–CBT paleotemperature proxy based on
557 branched tetraether membrane lipids in surface soils. Geochim. Cosmochim. Acta 96, 215–229,
558 http://dx.doi.org/10.1016/j.gca.2012.08.011.
559 Russell, J.M., Hopmans, E.C., Loomis, S.E., Liang, J. and Sinninghe Damsté, J.S. (2018) Distributions
560 of 5- and 6-methyl branched glycerol dialkyl glycerol tetraethers (brGDGTs) in East African lake
561 sediment: Effects of temperature, pH, and new lacustrine paleotemperature calibrations. Org. Geochem.
562 117, 56–69, https://doi.org/10.1016/j.orggeochem.2017.12.003.
563 Schouten, S., Hopmans, E.C., Baas, M., Boumann, H., Standfest, S., Könneke, M., Stahl, D.A. and
564 Sinninghe Damsté, J.S. (2008) Intact Membrane Lipids of "Candidatus Nitrosopumilus maritimus," a
565 Cultivated Representative of the Cosmopolitan Mesophilic Group I Crenarchaeota. Appl. Environ.
566 Microbiol. 74, 2433–2440, https://doi.org/10.1128/AEM.01709-07.
567 Schouten, S., Hopmans, E.C. and Sinninghe Damsté, J.S. (2013) The organic geochemistry of glycerol
568 dialkyl glycerol tetraether lipids: A review. Org. Geochem. 54, 19–61,
569 http://dx.doi.org/10.1016/j.orggeochem.2012.09.006.
570 Schouten, S., Huguet, C., Hopmans, E.C., Kienhuis, M.V.M. and Sinninghe Damsté, J.S. (2007)
571 Analytical methodology for TEX_{86} paleothermometry by high-performance liquid
572 chromatography/atmospheric pressure chemical ionization-mass spectrometry. Anal. Chem. 79, 2940–
573 2944, https://doi.org/10.1021/ac062339v.
574 Sinninghe Damsté, J.S. (2016) Spatial heterogeneity of sources of branched tetraethers in shelf systems:
575 The geochemistry of tetraethers in the Berau River delta (Kalimantan, Indonesia). Geochim. Cosmochim.
576 Acta 186, 13–31, https://doi.org/10.1016/j.gca.2016.04.033.
577 Sinninghe Damsté, J.S., Hopmans, E.C., Pancost, R.D., Schouten, S. and Geenevasen, J.A.J. (2000)
578 Newly discovered non-isoprenoid glycerol dialkylglycerol tetraether lipids in sediments. Cheminform
579 31, 1683–1684, https://doi.org/10.1002/chin.200048230.
580 Sinninghe Damsté, J.S., Ossebaar, J., Abbas, B., Schouten, S. and Verschuren, D. (2009) Fluxes and
581 distribution of tetraether lipids in an equatorial African lake: Constraints on the application of the TEX_{86}
582 palaeothermometer and BIT index in lacustrine settings. Geochim. Cosmochim. Acta 73, 4232–4249,
583 http://dx.doi.org/10.1016/j.gca.2009.04.022.
584 Sinninghe Damsté, J.S., Ossebaar, J., Schouten, S. and Verschuren, D. (2008) Altitudinal shifts in the

https://doi.org/10.5194/bg-2019-391
Preprint. Discussion started: 11 October 2019
© Author(s) 2019. CC BY 4.0 License.

branched tetraether lipid distribution in soil from Mt. Kilimanjaro (Tanzania): Implications for the MBT/CBT continental palaeothermometer. Org. Geochem. 39, 1072–1076, https://doi.org/10.1016/j.orggeochem.2007.11.011.

Sinninghe Damsté, J.S., Rijpstra, W.I., Hopmans, E.C., Weijers, J.W., Foesel, B.U., Overmann, J. and Dedysh, S.N. (2011) 13,16-Dimethyl octacosanedioic acid (iso-diabolic acid), a common membrane-spanning lipid of Acidobacteria subdivisions 1 and 3. Appl. Environ. Microbiol. 77, 4147–4154, https://doi.org/10.1128/aem.00466-11.

Sinninghe Damsté, J.S., Stefan, S., Hopmans, E.C., Duin, A.C.T., Van and Geenevasen, J.A.J. (2002) Crenarchaeol: the characteristic core glycerol dibiphytanyl glycerol tetraether membrane lipid of cosmopolitan pelagic crenarchaeota. J. Lipid Res. 43, 1641–1651, https://doi.org/10.1194/jlr.M200148-JLR200

Soelen, E.E.V., Kim, J.H., Santos, R.V., Dantas, E.L., Almeida, F.V.D., Pires, J.P., Roddaz, M. and Sinninghe Damsté, J.S. (2017) A 30 Ma history of the Amazon River inferred from terrigenous sediments and organic matter on the Ceará Rise. Earth Planet. Sci. Lett. 474, 40–48, https://doi.org/10.1016/j.epsl.2017.06.025.

Ta, K., Peng, X., Xu, H., Du, M., Chen, S., Li, J. and Zhang, C. (2019) Distributions and Sources of Glycerol Dialkyl Glycerol Tetraethers in Sediment Cores From the Mariana Subduction Zone. J. Geophys. Res. Biogeo. 124, 857–869, https://doi.org/10.1029/2018jg004748.

Taira, K., Kitagawa, S., Yamashiro, T. and Yanagimoto, D. (2004) Deep and bottom currents in the Challenger Deep, Mariana Trench, measured with super-deep current meters. J. Oceanogr. 60, 919–926, https://doi.org/10.1007/s10872-005-0001-y.

Takuro, N., Yoshihiro, T., Miho, H., Shigeru, S., Akiko, M., Osamu, K., Tohru, K., Junichi, M., Keisuke, K. and Naohiro, Y. (2015) Hadal biosphere: insight into the microbial ecosystem in the deepest ocean on Earth. Proc. Natl. Acad. Sci. USA 112, 1230–1236, https://doi.org/10.1073/pnas.1421816112.

Tian, J., Fan, L., Liu, H., Liu, J., Li, Y., Qin, Q., Gong, Z., Chen, H., Sun, Z., Zou, L., Wang, X., Xu, H., Bartlett, D., Wang, M., Zhang, Y.-Z., Zhang, X.-H. and Zhang, C.L. (2018) A nearly uniform distributional pattern of heterotrophic bacteria in the Mariana Trench interior. Deep Sea Res. Part I Oceanogr. Res. Pap. 142, 116–126, https://doi.org/10.1016/j.dsr.2018.10.002.

Tierney, J.E. and Russell, J.M. (2009) Distributions of branched GDGTs in a tropical lake system: Implications for lacustrine application of the MBT/CBT paleoproxy. Org. Geochem. 40, 1032–1036,

https://doi.org/10.5194/bg-2019-391
Preprint. Discussion started: 11 October 2019
© Author(s) 2019. CC BY 4.0 License.

615 http://dx.doi.org/10.1016/j.orggeochem.2009.04.014.

616 Turnewitsch, Robert, Falahat, Saeed, Stehlikova, Jirina, Oguri, Kazumasa, Glud and Ronnie, N. (2014)
617 Recent sediment dynamics in hadal trenches: Evidence for the influence of higher-frequency (tidal, near-
618 inertial) fluid dynamics. Deep Sea Res. Part I Oceanogr. Res. Pap. 90, 125–138,
619 https://doi.org/10.1016/j.dsr.2014.05.005.

620 Wang, H., Liu, W. and Lu, H. (2016) Appraisal of branched glycerol dialkyl glycerol tetraether-based
621 indices for North China. Org. Geochem. 98, 118–130, https://doi.org/10.1016/j.orggeochem.2016.05.013.

622 Wang, M., Zheng, Z., Zong, Y., Man, M. and Tian, L. (2019) Distributions of soil branched glycerol
623 dialkyl glycerol tetraethers from different climate regions of China. Sci. Rep. 9
624 https://doi.org/10.1038/s41598-019-39147-9.

625 Wang, M., Zong, Y., Zheng, Z., Man, M., Hu, J. and Tian, L. (2018) Utility of brGDGTs as temperature
626 and precipitation proxies in subtropical China. Sci. Rep. 8, https://doi.org/10.1038/s41598-41017-17964-
627 41590

628 Warden, L., Kim, J.H., Zell, C., Vis, G.J., Stigter, H.D., Bonnin, J. and Sinninghe Damsté, J.S. (2016)
629 Examining the provenance of branched GDGTs in the Tagus River drainage basin and its outflow into
630 the Atlantic Ocean over the Holocene to determine their usefulness for paleoclimate applications.
631 Biogeosciences 13, 5719–5738, https://doi.org/10.5194/bg-13-5719-2016.

632 Weber, Y., Jonge, C.D., Rijpstra, W.I.C., Hopmans, E.C., Stadnitskaia, A., Schubert, C.J., Lehmann, M.F.,
633 Sinninghe Damsté, J.S. and Niemann, H. (2015) Identification and carbon isotope composition of a novel
634 branched GDGT isomer in lake sediments: Evidence for lacustrine branched GDGT production.
635 Geochim. Cosmochim. Acta 154, 118–129, https://doi.org/10.1016/j.gca.2015.01.032.

636 Weber, Y., Sinninghe Damsté, J.S., Zopfi, J., De Jonge, C., Gilli, A., Schubert, C.J., Lepori, F., Lehmann,
637 M.F. and Niemann, H. (2018) Redox-dependent niche differentiation provides evidence for multiple
638 bacterial sources of glycerol tetraether lipids in lakes. Proc. Natl. Acad. Sci. USA 115, 10926,
639 https://doi.org/10.1073/pnas.1805186115.

640 Weijers, J.W.H., Schefuß, E., Kim, J.-H., Sinninghe Damsté, J.S. and Schouten, S. (2014) Constraints on
641 the sources of branched tetraether membrane lipids in distal marine sediments. Org. Geochem. 72, 14–
642 22, http://dx.doi.org/10.1016/j.orggeochem.2014.04.011.

643 Weijers, J.W.H., Schefuß, E., Schouten, S. and Sinninghe Damsté, J.S. (2007a) Coupled thermal and
644 hydrological evolution of tropical Africa over the last deglaciation. Science 315, 1701–1704,

https://doi.org/10.5194/bg-2019-391
Preprint. Discussion started: 11 October 2019
© Author(s) 2019. CC BY 4.0 License.

https://doi.org/10.1126/science.1138131.

Weijers, J.W.H., Schouten, S., Donker, J.C.V.D., Hopmans, E.C. and Sinninghe Damsté, J.S. (2007b) Environmental controls on bacterial tetraether membrane lipid distribution in soils. Geochim. Cosmochim. Acta 71, 703–713, https://doi.org/10.1016/j.gca.2006.10.003.

Weijers, J.W.H., Schouten, S., Spaargaren, O.C. and Sinninghe Damsté, J.S. (2006) Occurrence and distribution of tetraether membrane lipids in soils: Implications for the use of the TEX86 proxy and the BIT index. Org. Geochem. 37, 1680–1693, http://dx.doi.org/10.1016/j.orggeochem.2006.07.018.

Wu, W., Zhao, L., Pei, Y., Ding, W., Yang, H. and Xu, Y. (2013) Variability of tetraether lipids in Yellow River-dominated continental margin during the past eight decades: Implications for organic matter sources and river channel shifts. Org. Geochem. 60, 33–39, https://doi.org/10.1016/j.orggeochem.2013.04.014.

Xiao, W., Wang, Y., Zhou, S., Hu, L., Yang, H. and Xu, Y. (2016) Ubiquitous production of branched glycerol dialkyl glycerol tetraethers (brGDGTs) in global marine environments: A new source indicator for brGDGTs. Biogeosciences 13, 5883–5894, https://doi.org/10.5194/bg-13-5883-2016.

Xiao, W., Wang, Y., Liu, Y., Zhang, X., Shi, L., Fang, J. and Xu, Y. (2019) Predominance of hexamethylated 6-methyl branched glycerol dialkyl glycerol tetraethers in the Mariana Trench: Source and environmental implication. Figshare, https://doi.org/10.6084/m9.figshare.9896120.v1.

Xiao, W., Xu, Y., Ding, S., Wang, Y., Zhang, X., Yang, H., Wang, G. and Hou, J. (2015) Global calibration of a novel, branched GDGT-based soil pH proxy. Org. Geochem. 89–90, 56–60, http://dx.doi.org/10.1016/j.orggeochem.2015.10.005.

Xie, S., Liu, X.L., Schubotz, F., Wakeham, S.G. and Hinrichs, K.U. (2014) Distribution of glycerol ether lipids in the oxygen minimum zone of the Eastern Tropical North Pacific Ocean. Org. Geochem. 71, 60–71, https://doi.org/10.1016/j.orggeochem.2014.04.006.

Xu, Y., Ge, H. and Fang, J. (2018) Biogeochemistry of hadal trenches: Recent developments and future perspectives. Deep Sea Res. Part II Top. Stud. Oceanogr. 155, 19–26, https://doi.org/10.1016/j.dsr2.2018.10.006.

Yang, H., Lü, X., Ding, W., Lei, Y., Dang, X. and Xie, S. (2015) The 6-methyl branched tetraethers significantly affect the performance of the methylation index (MBT') in soils from an altitudinal transect at Mount Shennongjia. Org. Geochem. 82, 42–53, https://doi.org/10.1016/j.orggeochem.2015.02.003.

Yang, H., Pancost, R.D., Dang, X., Zhou, X., Evershed, R.P., Xiao, G., Tang, C., Gao, L., Guo, Z. and

https://doi.org/10.5194/bg-2019-391
Preprint. Discussion started: 11 October 2019
© Author(s) 2019. CC BY 4.0 License.

675 Xie, S. (2014) Correlations between microbial tetraether lipids and environmental variables in Chinese
676 soils: Optimizing the paleo-reconstructions in semi-arid and arid regions. Geochim. Cosmochim. Acta
677 126, 49–69, http://dx.doi.org/10.1016/j.gca.2013.10.041.
678 Zang, J., Lei, Y. and Yang, H. (2018) Distribution of glycerol ethers in Turpan soils: implications for use
679 of GDGT-based proxies in hot and dry regions. Front. Earth Sci., https://doi.org/10.1007/s11707-11018-
680 10722-z
681 Zell, C., Kim, J.-H., Moreira-Turcq, P., Abril, G., Hopmans, E.C., Bonnet, M.-P., Sobrinho, R.L. and
682 Sinninghe Damsté, J.S. (2013) Disentangling the origins of branched tetraether lipids and crenarchaeol
683 in the lower Amazon River: Implications for GDGT-based proxies. Limnol. Oceanogr. 58, 343–353,
684 https://doi.org/10.4319/lo.2013.58.1.0343.
685 Zell, C., Kim, J.H., Balsinha, M., Dorhout, D., Fernandes, C., Baas, M. and Sinninghe Damsté, J.S.
686 (2014a) Transport of branched tetraether lipids from the Tagus River basin to the coastal ocean of the
687 Portuguese margin: consequences for the interpretation of the MBT'/CBT paleothermometer.
688 Biogeosciences 11, 5637–5655, https://doi.org/10.5194/bg-11-5637-2014.
689 Zell, C., Kim, J.H., Hollander, D., Lorenzoni, L., Baker, P., Silva, C.G., Nittrouer, C. and Sinninghe
690 Damsté, J.S. (2014b) Sources and distributions of branched and isoprenoid tetraether lipids on the
691 Amazon shelf and fan: Implications for the use of GDGT-based proxies in marine sediments. Geochim.
692 Cosmochim. Acta 139, 293–312, https://doi.org/10.1016/j.gca.2014.04.038.
693 Zhang, C., Wang, J., Wei, Y., Zhu, C., Huang, L. and Dong, H. (2012) Production of branched tetraether
694 lipids in the lower Pearl River and estuary: effects of extraction methods and impact on bGDGT proxies.
695 Front. Microbiol. 2 https://doi.org/10.3389/fmicb.2011.00274.
696 Zhu, C., Weijers, J.W.H., Wagner, T., Pan, J.M., Chen, J.F. and Pancost, R.D. (2011) Sources and
697 distributions of tetraether lipids in surface sediments across a large river-dominated continental margin.
698 Org. Geochem. 42, 376–386, https://doi.org/10.1016/j.orggeochem.2011.02.002.
699
700

https://doi.org/10.5194/bg-2019-391
Preprint. Discussion started: 11 October 2019
© Author(s) 2019. CC BY 4.0 License.

Biogeosciences Discussions Open Access EGU

701 **Table 1.** Organic carbon (OC) content, total nitrogen (TN) content, molar ratio of OC/TN and stable
702 carbon isotopic composition ($\delta^{13}C$) in the Mariana Trench sediments

703

Sample ID	Depth (cm)	OC (wt. %)	TN (wt. %)	OC/TN (mol/mol)	$\delta^{13}C$ (‰)
MT1	0-2	0.31	0.05	6.52	–20.02
MT2.5	2-3	0.27	0.05	6.05	–19.66
MT3.5	3-4	0.29	0.05	6.85	–19.55
MT4.5	4-5	0.27	0.05	5.78	–19.84
MT5.5	5-6	0.29	0.06	6.13	–19.94
MT6.5	6-7	0.30	0.06	5.62	–19.47
MT7.5	7-8	0.27	0.04	7.27	-19.54
MT8.5	8-9	0.29	0.05	6.93	–19.82
MT9.5	9-10	0.28	0.04	7.74	–20.09
MT10.5	10-11	0.26	0.04	8.34	–20.27

704

705

https://doi.org/10.5194/bg-2019-391
Preprint. Discussion started: 11 October 2019
© Author(s) 2019. CC BY 4.0 License.

Biogeosciences Discussions Open Access EGU

706 **Table 2.** Fractional abundance and concentration of brGDGTs and crenarchaeol (cren) in the Mariana Trench sediments.

Sample ID	Ia (%)	Ib (%)	Ic (%)	IIa (%)	IIa' (%)	IIb (%)	IIb' (%)	IIc (%)	IIc' (%)	IIIa (%)	IIIa' (%)	IIIb (%)	IIIb' (%)	IIIc (%)	IIIc' (%)	BrGDGTs (ng/g)	Cren (ng/g)
MT1	13.6	2.7	1.5	0.0	10.4	0.0	0.0	0.0	0.0	0.0	71.8	0.0	0.0	0.0	0.0	18.4	353.3
MT2.5	13.5	2.4	1.6	0.0	12.1	0.0	1.3	0.0	0.0	0.0	69.0	0.0	0.0	0.0	0.0	14.7	426.7
MT3.5	11.1	1.4	0.6	0.0	9.5	0.0	0.6	0.0	0.0	0.0	76.2	0.0	0.6	0.0	0.0	16.4	659.8
MT4.5	14.2	1.4	0.9	0.0	9.2	0.0	0.4	0.0	0.0	0.0	73.9	0.0	0.0	0.0	0.0	12.6	515.4
MT5.5	11.1	2.0	0.8	0.0	10.3	0.0	0.8	0.0	0.0	0.0	75.0	0.0	0.0	0.0	0.0	15.1	622.7
MT6.5	11.2	2.1	0.9	0.0	9.1	0.0	0.0	0.0	0.0	0.0	76.0	0.0	0.8	0.0	0.0	20.1	667.2
MT7.5	13.4	1.5	1.0	0.0	11.3	0.0	1.2	0.0	0.0	0.0	71.5	0.0	0.0	0.0	0.0	12.7	551.8
MT8.5	13.0	2.2	1.1	0.0	12.7	0.0	0.0	0.0	0.0	0.0	70.9	0.0	0.0	0.0	0.0	13.0	585.1
MT9.5	11.8	2.0	0.7	0.0	9.2	0.0	0.0	0.0	0.0	0.0	76.3	0.0	0.0	0.0	0.0	11.5	450.6
MT10.5	11.8	1.8	1.0	0.0	10.6	0.0	1.0	0.0	0.4	0.0	73.3	0.0	0.0	0.0	0.0	14.3	498.3

707

https://doi.org/10.5194/bg-2019-391
Preprint. Discussion started: 11 October 2019
© Author(s) 2019. CC BY 4.0 License.

Biogeosciences
Discussions
Open Access
EGU

708 **Figure 1.** Location of the samples in this study. Red, blue, green, orange and pink circles indicate
709 globally distributed soil, river, lake, peat and marine samples, respectively. Black star denotes the
710 sediment core in the Mariana Trench. The detailed information is provided in supplementary
711 material.

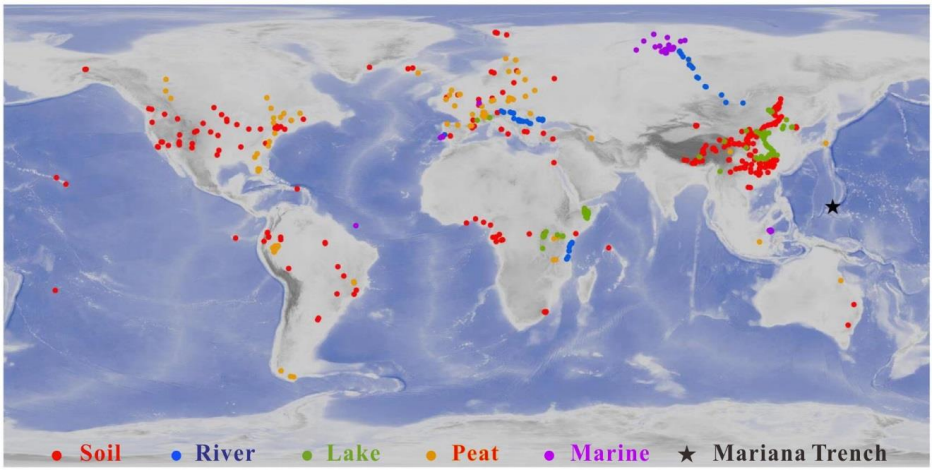

712

https://doi.org/10.5194/bg-2019-391
Preprint. Discussion started: 11 October 2019
© Author(s) 2019. CC BY 4.0 License.

713 **Figure 2.** Chemical structures of brGDGTs and crenarchaeol.

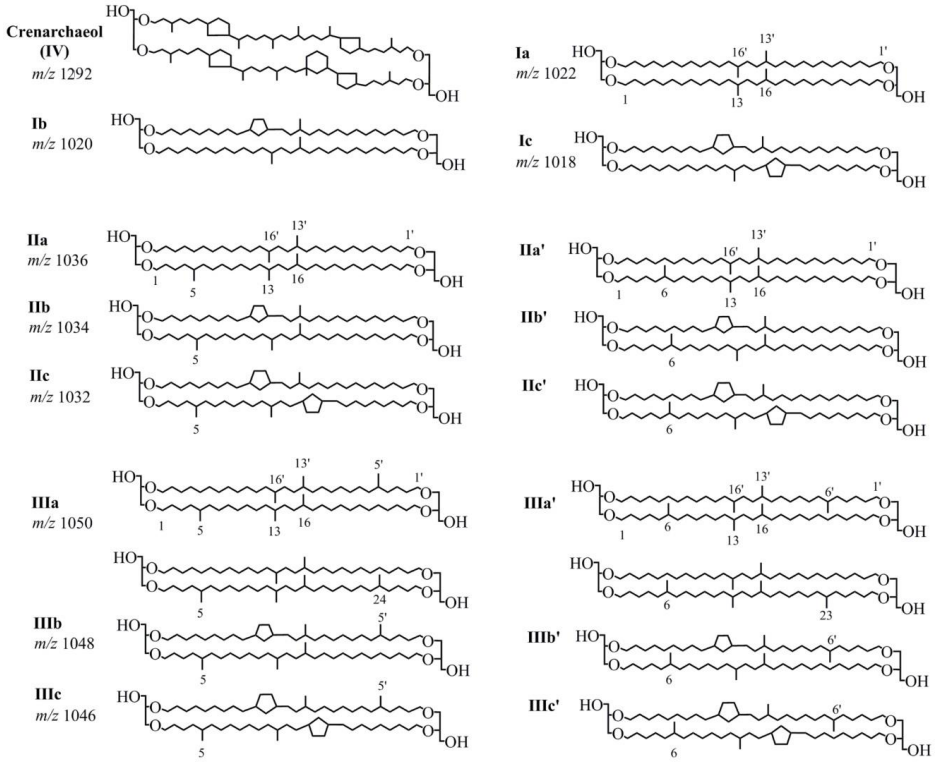

https://doi.org/10.5194/bg-2019-391
Preprint. Discussion started: 11 October 2019
© Author(s) 2019. CC BY 4.0 License.

714 **Figure 3.** Extracted ion chromatograms (EICs) of m/z 1050 (left) and m/z 1036 (right) showing
715 separation of 5-methyl and 6-methyl brGDGTs in soil (top), Mariana Trench sediment (middle) and
716 combined soil and sediment (bottom).

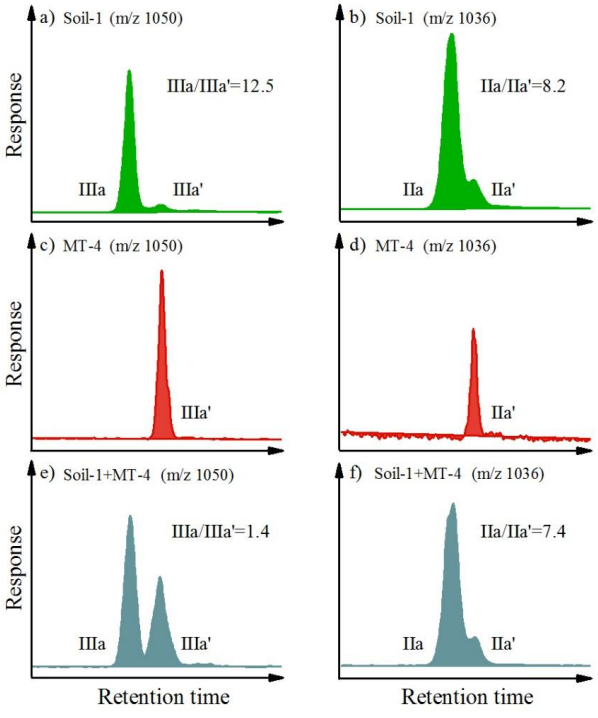

717

https://doi.org/10.5194/bg-2019-391
Preprint. Discussion started: 11 October 2019
© Author(s) 2019. CC BY 4.0 License.

Biogeosciences
Discussions
Open Access
EGU

718 **Figure 4.** Plot of $\delta^{13}C$ versus TN/OC for core sediments from the Mariana Trench (MT). Included
719 in this graph are different compositional ranges of C_3 vascular plants, C_4 vascular plants, bacteria,
720 river and estuary phytoplankton and marine phytoplankton sources. The compositional range of
721 different end members was cited from Goñi et al. (2006) and Hu et al. (2016). The red stars and
722 green stars denote data from this study and Luo et al. (2017), respectively.

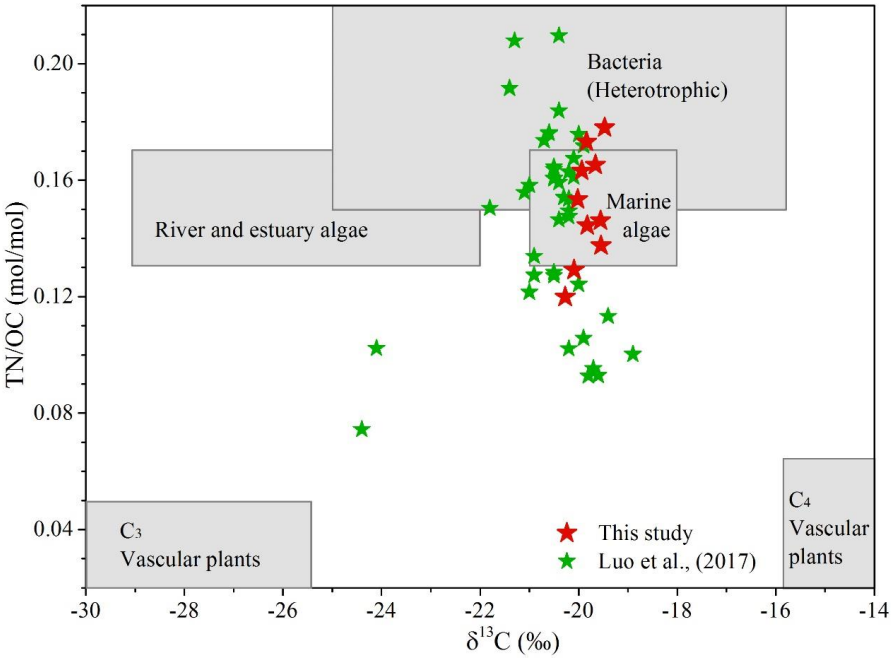

723
724
725

https://doi.org/10.5194/bg-2019-391
Preprint. Discussion started: 11 October 2019
© Author(s) 2019. CC BY 4.0 License.

726 **Figure 5.** Comparisons of distribution of 15 brGDGT compounds in soil (n = 634), peat (n = 473),

727 river (n = 88), lake (n = 410), marine (n = 415) and Mariana Trench (n = 11) samples.

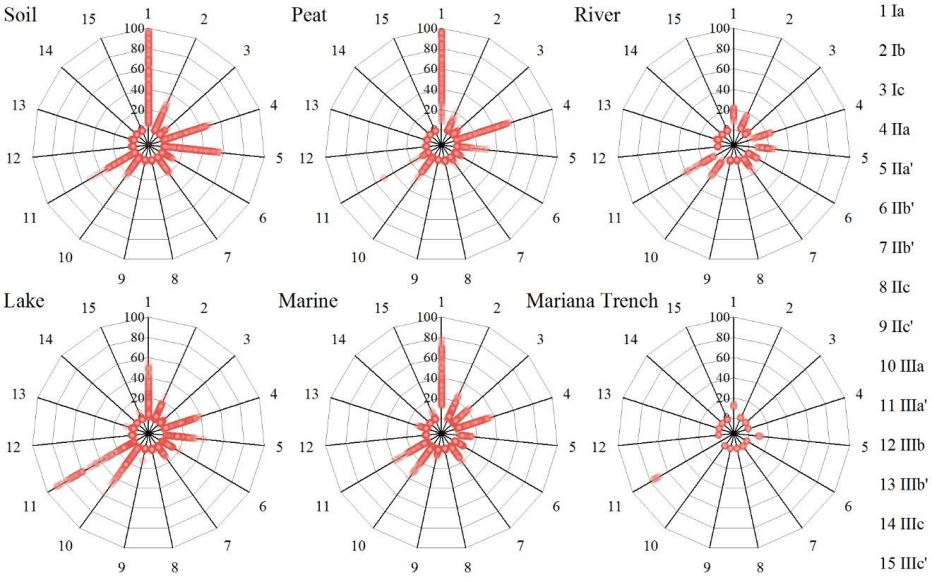

728

https://doi.org/10.5194/bg-2019-391
Preprint. Discussion started: 11 October 2019
© Author(s) 2019. CC BY 4.0 License.

Biogeosciences
Discussions
Open Access
EGU

729 **Figure 6.** Relationship between the (IIIa+IIIa')/(IIa+IIa') index and the BIT index of the Mariana
730 Trench sediments (red star) and globally distribute soil (green circle) and marine samples (blue
731 square). The dashed lines represent the upper limit of production in the terrestrial realm and the
732 lower limit of production in the marine realm defined by Xiao et al. (2016).

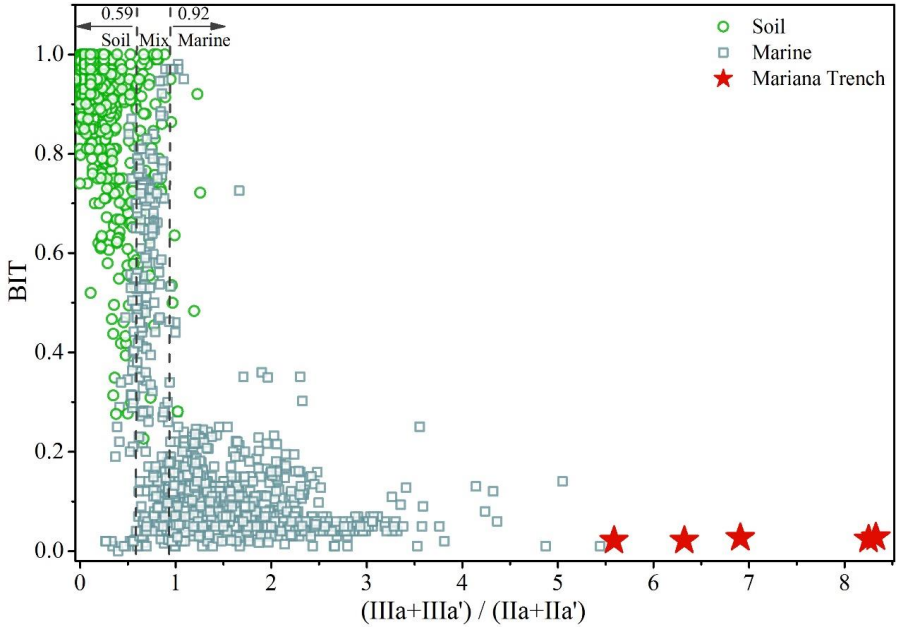

733

734

https://doi.org/10.5194/bg-2019-391
Preprint. Discussion started: 11 October 2019
© Author(s) 2019. CC BY 4.0 License.

735 **Figure 7.** Scatterplots of the a) CBT', b) IBT, c) CBT_{5me} and d) $\#rings_{tetra}$ index versus measured
736 pH of globally distributed soils. The black solid line and dashed line denote the linear calibration
737 line and associated confidence intervals of 95%. The gray block (a) represents corresponding values
738 of the Mariana Trench sediment in this study.

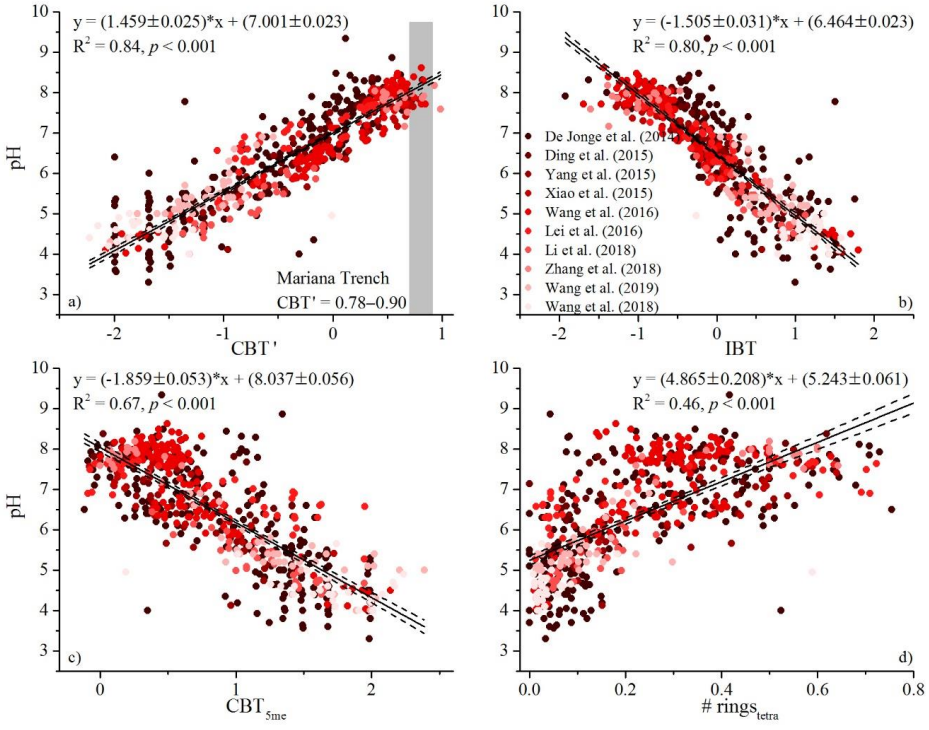

739

740

741

https://doi.org/10.5194/bg-2019-391
Preprint. Discussion started: 11 October 2019
© Author(s) 2019. CC BY 4.0 License.

742 **Figure 8.** Vertical profiles of a) the proportion of GDGT-IIIa', b) $\delta^{13}C$ and c) BIT index of a marine
743 sediment core from the North Sea Basin (Dearing Crampton-flood et al., 2018). Vertical profiles of
744 d) the proportion of GDGT-IIIa', e) $\delta^{13}C$, f) BIT index of a marine sediment core from the Kara Sea
745 (De Jonge et al., 2016). Spatial distribution patterns of g) average distribution of brGDGTs and h)
746 BIT index in the transect from the land to the ocean off the Portuguese coast (river floodplain,
747 mudbelt, Lisbon canyon head and lower Setúbal canyon) (Warden et al., 2016). Isosurface plots of
748 i) BIT index, j) $\delta^{13}C$ and k) the proportion of GDGT-IIIa' of the surface sediments from the Berau
749 River delta (Sinninghe Damsté, 2016).
750

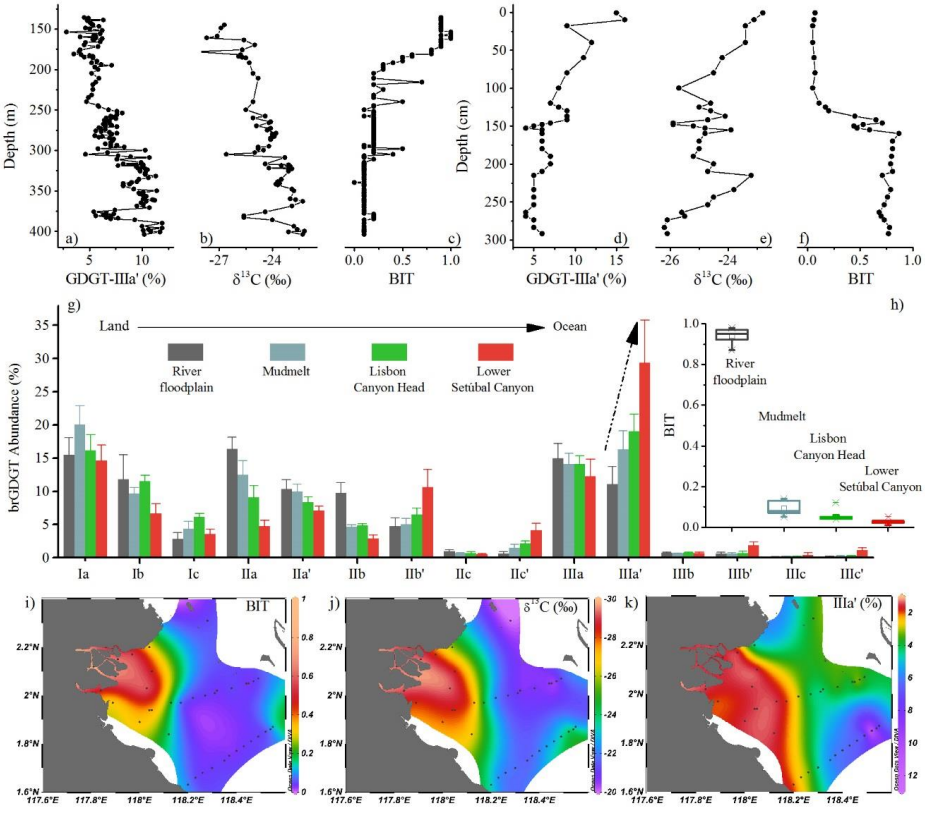

751

https://doi.org/10.5194/bg-2019-391
Preprint. Discussion started: 11 October 2019
© Author(s) 2019. CC BY 4.0 License.

752 **Figure 9** a) Ternary diagram showing the fractional abundances of tetra-, penta- and hexamethylated
753 brGDGTs. b) and d) Cross plots of the fractional abundances of tetramethylated brGDGTs versus
754 hexa- and pentamethylated brGDGTs, respectively. c) Cross plots of the fractional abundances of
755 pentamethylated brGDGTs versus hexamethylated brGDGTs. The compiled dataset (Supplementary)
756 includes globally distributed soil, peat, lake, river and marine samples, as well as the Mariana Trench
757 sediments.

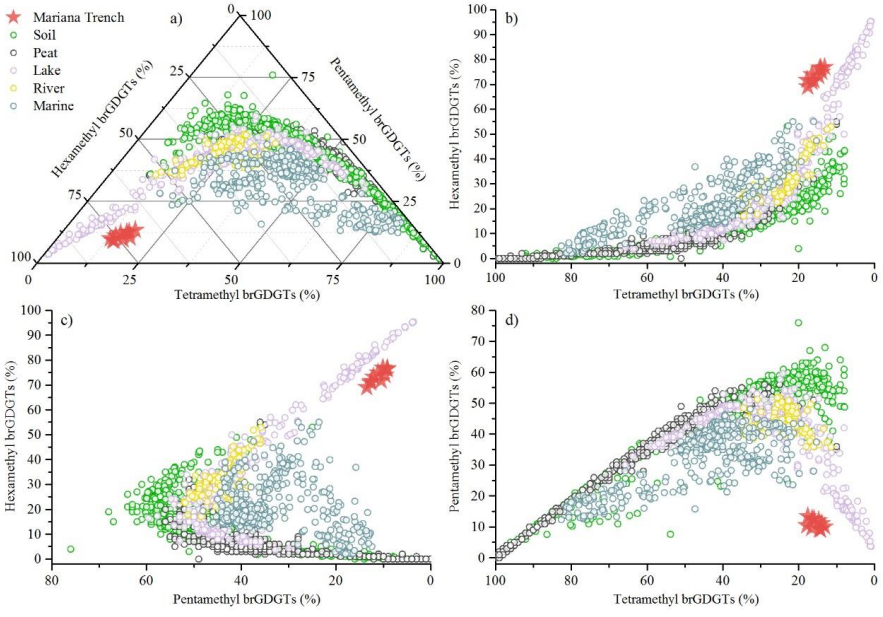

758

759

760

https://doi.org/10.5194/bg-2019-391
Preprint. Discussion started: 11 October 2019
© Author(s) 2019. CC BY 4.0 License.

Biogeosciences
Discussions
Open Access
EGU

761 **Figure 10** Scatterplots of the (IIIa+IIIa')/(IIa+IIa') index versus the proportion of brGDGT-IIIa' of
762 globally distributed soils and marine sediments. The solid, dashed and dotted line denotes the Linear
763 fit, 95% confidence band and 95% prediction band of concatenated data, respectively. The number
764 of samples, slope, R^2 and *p* values of calibration for the global distributed soils, marine sediments
765 and Mariana Trench sediments are given.

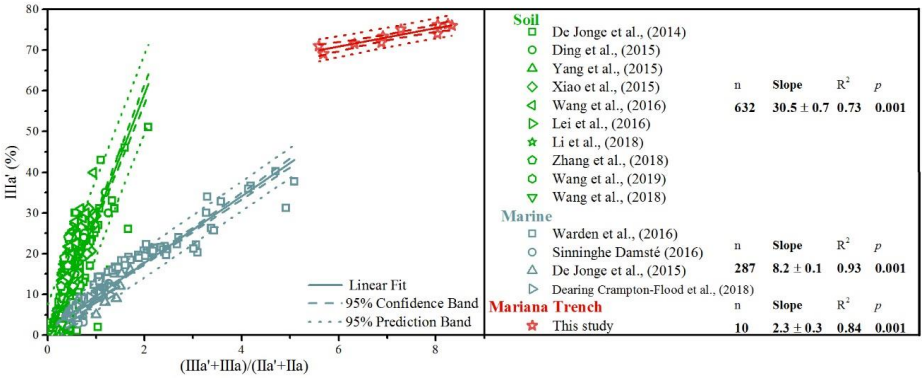

766